

Sequence-based Design of Kinase Inhibitors Applicable for Therapeutics and Target Identification*[§]

Received for publication, June 25, 2003, and in revised form, October 6, 2003
Published, JBC Papers in Press, October 21, 2003, DOI 10.1074/jbc.M306723200

Masha Y. Niv[‡], Hila Rubin[‡], Jacob Cohen[‡], Lilia Tsurulnikov[‡], Tamar Licht[‡],
Adi Peretzman-Shemer[‡], Einat Cna'an[‡], Alexander Tartakovsky[‡], Ilan Stein[‡], Shira Albeck[‡],
Irina Weinstein[‡], Mirela Goldenberg-Furmanov[‡], Dror Tobi[‡], Einat Cohen[¶], Morris Laster[‡],
Shmuel A. Ben-Sasson[¶], and Hadas Reuveni[‡]

From [‡]Keryx Biopharmaceuticals, 15 Yad-Haruzim St., Jerusalem 93420, Israel and the [¶]Department of Experimental Medicine and Cancer Research, The Hebrew University-Hadassah Medical School, P. O. Box 12272 Jerusalem, Israel

A platform for specifically modulating kinase-dependent signaling using peptides derived from the catalytic domain of the kinase is presented. This technology, termed KinAceTM, utilizes the canonical structure of protein kinases. The targeted regions (subdomain V and subdomains IX and X) are analyzed and their sequence, three-dimensional structure, and involvement in protein-protein interaction are highlighted. Short myristoylated peptides were derived from the target regions of the tyrosine kinases c-Kit and Lyn and the serine/threonine kinases 3-phosphoinositide-dependent kinase-1 (PDK1) and Akt/protein kinase B (PKB). For each kinase an active designer peptide is shown to selectively inhibit the signaling of the kinase from which it is derived, and to inhibit cancer cell proliferation in the micromolar range. This technology emerges as an applicable tool for deriving sequence-based selective inhibitors for a broad range of protein kinases as hits that may be further developed into drugs. Moreover, it enables identification of novel kinase targets for selected therapeutic indications as demonstrated in the KinScreen application.

Protein kinases are important drug targets for oncologic, immunologic, and metabolic disorders. The development of selective protein kinase inhibitors is widely considered a promising approach to drug development. The common strategy, which has led to the development of drugs, such as Gleevec and Iressa (1), is to target the ATP binding site (1–3). Other approaches include substrate mimicking inhibitors (4–9), bi-substrate analogs that target both the ATP and the acceptor binding sites (10), and molecules that target the Src homology 2 domain (11). The KinAceTM (12) approach presented in this article is based upon deriving short peptides from specific regions in the catalytic domain of the kinase that are implicated in kinase-substrate interactions. The KinAceTM peptides mimic regions of the kinase and therefore compete with the kinase for binding to the substrate (or to other modulators of the kinase), and subsequently abrogate the kinase-dependent signaling.

Several other groups have used peptides to disrupt protein-protein interactions and thus modulate kinase signaling. In con-

trast to our technology, which derives the peptides from the catalytic domain of the kinase, others have derived inhibitory peptides from the substrates (7), pseudosubstrate (13), regulators interacting with the kinase (14–17), or from non-catalytic domains of the kinase participating in substrate binding (11, 18). One of the unique characteristics of the KinAceTM technology is that the regions from which the inhibitory peptides are derived share conserved structural patterns in all kinases. Evidence from the literature supports a potential role for these regions in substrate binding (19–22). Our technology suggests a general recipe for generating inhibitors of kinase-dependent signaling, applicable to any kinase. To enable permeation of peptides into cells researchers conjugated peptides to membrane penetrating sequences (14, 18, 23) or to fatty acids (myristate (7, 13, 18) or stearate (17)). In our hands, myristoylation works very efficiently as was already demonstrated earlier (24, 25).

This paper summarizes data that point to the pivotal role of the KinAceTM regions of various kinases, in substrate binding. The sequence and structural characteristics of these regions are analyzed utilizing published three-dimensional structures of kinase-substrate complexes and mutational studies, as well as accessibility and variability of residues in these regions. We derive myristoylated peptides based on the KinAceTM regions of selected kinases and show that they selectively inhibit kinase-dependent phosphorylation in cellular or cell-free assays. We further show the inhibitory effects of these peptides on proliferation of cancer cells. We thus demonstrate the applicability of the KinAceTM approach for systematic derivation of selective kinase inhibitors, and the possibility of using the resulting peptides as lead compounds for optimization into potential drugs. Finally, we describe the KinScreen application, which enables identification of novel links between kinases and therapeutic indications. Specifically, we exemplify how a known kinase, Lyn, was identified as a novel target for the treatment of solid tumors.

EXPERIMENTAL PROCEDURES

Peptides—Peptides (purity >85%) were synthesized by Fmoc solid phase peptide synthesis and purified by reverse phase-high performance liquid chromatography, by Novetide Ltd. (Haifa, Israel) or Genemed Synthesis Inc. (San Francisco, CA). Identity and purity were confirmed by high performance liquid chromatography mass spectroscopy.

Me₂SO based formulations used were the following. Me₂SO, the peptide was dissolved in 100% Me₂SO at 10 mM concentration. Me₂SOT, the peptide was dissolved in 100% Me₂SO at 10 mM concentration and heated at 100 °C for 30 min, and for DMSOTbi, 40 μl of 10 mM peptide dissolved in Me₂SO were added to 160 μl of 2 M ammonium bicarbonate solution and heated at 100 °C for 40 min until no evaporation was detected. For the cell proliferation assay peptides were further diluted

* The costs of publication of this article were defrayed in part by the payment of page charges. This article must therefore be hereby marked "advertisement" in accordance with 18 U.S.C. Section 1734 solely to indicate this fact.

[§] The on-line version of this article (available at <http://www.jbc.org>) contains Appendix A, Appendix B, and Refs. 94–100.

[‡] Both authors contributed equally to this work.

[¶] To whom correspondence should be addressed. Tel.: 972-2-6732910; E-mail: hadas@keryx.com.

in 0.1% bovine serum albumin (BSA)¹ in PBS, pH 7.4 (BSA-PBS).

Cell Culture and Cell Proliferation Assay—All cell lines are of human origin. Hormone refractory prostate cancer cell lines DU-145 and PC-3, mammary gland breast carcinoma cell lines MCF-7 and MDA-MB-231, and epithelial colorectal adenocarcinoma cell line HT-29 and human NCI-H526 small cell lung carcinoma cells were obtained from American Type Culture Collection (ATCC). Ovarian carcinoma cell line A2780 was purchased from the European Collection of Cell Cultures. Cells were grown and treated in RPMI 1640 (standard or Dutch modification) or Dulbecco's modified Eagle's medium containing 10% fetal calf serum, 2 mM glutamine, 100 units/ml penicillin, and 0.1 mg/ml streptomycin (all reagents for cell culture were purchased from Biological Industries Bet-Haemek Ltd., Israel).

For the cell proliferation assay $3.6\text{--}7.2 \times 10^3$ cells/well were seeded in 96-well tissue culture plates (180 μ l/well). The inhibitors were added 3 h later to allow cell adhesion to the plates. The peptides were prepared as stock solutions in Me₂SO-based formulations as described above (except for KRX-014_{H151} that was prepared in AM159 formulation as detailed below). The stock solution was diluted to 100 μ M in PBS containing 0.1% BSA and further 1:1 dilutions were made while retaining a constant vehicle concentration. Aliquots (20 μ l) were dispersed in triplicates into the cell-containing wells, either of peptide dilutions, vehicle, or non-treated (BSA-PBS). Plates are incubated at 37 °C in a 5% CO₂ humidified incubator for 3–4 days, fixed in 4% buffered formaldehyde solution for 2 h, washed with 0.1 M sodium borate buffer, pH 8.5, and stained with 1% methylene blue dissolved in 0.1 M borate buffer solution for 10 min. Excess dye was washed out and cell-bound dye was eluted with 200 μ l/well of 0.1 M HCl. The optical density value was read at 595 nm in the Labsystems Multiscan RC enzyme-linked immunosorbent assay plate reader. The data was analyzed in Microsoft Excel, using the vehicle control as 100% proliferation. The vehicle had no significant effect on cell proliferation.

Immunoblotting—Samples of cell-free kinase assays or aliquots of cell extracts containing equal amounts of protein were resolved by SDS-PAGE and electroblotted onto nitrocellulose filters. Membranes were blocked with blocking solution containing either 5% low fat milk or 3% BSA in TBST (25 mM Tris, pH 7.4, 140 mM NaCl, 0.2% Tween 20), incubated with primary antibodies (Abs) overnight at 4 °C, and then with horseradish peroxidase-conjugated goat anti-rabbit or donkey anti-mouse secondary Abs (Jackson ImmunoResearch Laboratories) for 1 h at room temperature. Immunoreactive bands were visualized using the enhanced chemiluminescence (ECL) detection system (Pierce), and quantified using ImageJ software version 1.26t.

Cloning and Expression of GST-Syk—The entire Syk open reading frame was generated by reverse transcriptase-PCR (accession number L28824) and cloned into pGEX-2T (Amersham Biosciences) as a glutathione S-transferase (GST) fusion of Syk. The plasmid was verified by sequencing. Expression of GST-Syk in *Escherichia coli* BL21 Lys was induced by 0.1 mM isopropyl- β -D-thiogalactopyranoside (IPTG) at an A₆₀₀ of 0.6, and allowed to grow at 26 °C for 6 h. Bacterial cells were sonicated in PBS supplemented with 5 mM EDTA, 5 mM dithiothreitol, and bacterial protease inhibitor mixture (Sigma) on ice, prior to centrifugation for 10 min at 14,000 rpm at 4 °C. Soluble GST-Syk was purified with GSTrapTMFF (Amersham Pharmacia Biotech) using an AKTAdesign (Amersham Biosciences). GST-Syk eluted with 40 mM glutathione yielding 90% pure protein. Protein concentration was determined by absorbance at 280 nm.

Lyn-Syk Cell-free Kinase Assay—Each reaction contained a peptide of interest dissolved in 1% Me₂SO at a concentration indicated in the figure, 98 ng of GST-Syk and 27 ng of active His-tagged recombinant human Lyn (Panvera) in reaction buffer (50 mM Tris, pH 7.5, 10 mM MgCl₂, 1 mM dithiothreitol, and 0.1 mM sodium orthovanadate). The mixtures were agitated at 900 rpm for 20 min at 30 °C, and reactions were initiated by the addition of 100 μ M ATP, and maintained for 10 min under the same conditions. Reactions were stopped by the addition of SDS sample buffer, separated on SDS-PAGE, and probed with anti-phosphotyrosine (anti-Tyr(P)), 4G10, Upstate) monoclonal antibodies (mAb) followed by reprobing with anti-Syk polyclonal Abs (Santa Cruz Biotechnology).

Cloning and Expression of Lyn—The entire Lyn open reading frame was generated by reverse transcriptase-PCR (accession number M16038), and cloned into pET-21b (Novagen). Kinase-dead Lyn was prepared by the mutation of lysine to leucine at position 275 (designated Lyn-K275L). *In vitro* mutagenesis was performed using GeneEditor *in vitro* site-directed mutagenesis system (Promega). Plasmid constructs were verified by sequencing. Expression of Lyn-K275L in *E. coli* BL21 Lys was induced by 0.1 mM isopropyl- β -D-thiogalactopyranoside at an A₆₀₀ of 0.6, and allowed to grow at 26 °C for 4 h. The bacteria were lysed as described for GST-Syk. Lyn-K275L was expressed as inclusion bodies, which were dissolved in 20 mM Tris, pH 10.3, containing 3 M urea for 1 h at room temperature. The denatured soup was centrifuged for 5 min at 14,000 rpm and the supernatant was subjected to three dialysis steps at 4 °C: against 20 mM Tris, pH 9.0 and 8.5, each containing 5% glycerol and 100 mM NaCl, and finally against 20 mM Tris, pH 7.5. The refolded protein was centrifuged for 5 min at 14,000 rpm yielding 95% pure protein with no further purification steps. Protein concentration was determined by absorbance at 280 nm.

Lyn Cell-free Transphosphorylation Assay—Each reaction contained a peptide of interest dissolved in 1% Me₂SO at the concentration indicated in the figure, 720 ng of Lyn-K275L, 13.5 ng of active His-tagged recombinant human Lyn (Panvera) in reaction buffer. The mixtures were treated as described for the Lyn-Syk assay, but maintained for 15 min following addition of ATP. Western blots were probed with anti-Tyr(P) mAb, followed by reprobing with anti-Lyn Abs (Santa Cruz Biotechnology).

Src Cell-free Transphosphorylation Assay—Each reaction contained peptides dissolved in 1% Me₂SO and 220 ng of Src (Biomol Research Laboratories) in reaction buffer. The mixtures were agitated at 800 rpm for 20 min at 30 °C, reactions were initiated by the addition of 100 μ M ATP, and agitation was maintained for 10 min. Reactions were terminated by SDS sample buffer and samples were separated on SDS-PAGE and probed with anti-Tyr(P) mAb, followed by reprobing with anti-Src Abs (Santa Cruz Biotechnology).

PKB-GSK3 Cell-free Kinase Assay—DU-145 cells were serum-starved overnight and lysed at 4 °C in mild lysis buffer (50 mM Tris, pH 7.5, 75 mM NaCl, 1% Nonidet P-40, 2 mM EDTA, 50 mM NaF, 5 mM NaPP₃, 0.2 mM Na₃VO₄, and protease inhibitor mixture (Aldrich-Sigma)). Samples were centrifuged at 14,000 rpm for 20 min at 4 °C, and supernatants were subjected to immunoprecipitation of glycogen synthetase kinase 3 (GSK3) by 2 μ g/sample anti-GSK3 Ab (Transduction Laboratories) and 15 μ l/sample immobilized protein G (Pierce) at 4 °C for 4 h. Immunoprecipitates were washed twice with cold mild lysis buffer and twice with cold reaction buffer II (25 mM Tris, pH 7.5, 10 mM MgCl₂, 2 mM dithiothreitol, 5 mM β -glycerophosphate, and 0.1 mM sodium orthovanadate). Reaction buffer containing 120 ng/sample recombinant active Akt1/PKB α (Upstate Biotechnology) and either peptides at the indicated concentrations or vehicle (0.1% Me₂SO and 0.9% ethanol in DDW) were added. Samples were rotated 1400 rpm at 30 °C for 20 min, prior to the addition of ATP to a final concentration of 100 μ M for an additional 5-min incubation. Reactions were terminated by SDS sample buffer and samples were separated by SDS-PAGE and probed with anti-phospho-GSK3 Ab (Cell Signaling Technology) followed by anti-GSK3 Ab (Transduction Laboratories).

Transphosphorylation of c-Kit and NCI-H526 Cell Proliferation—NCI-H526 cells were grown in RPMI 1640 media containing 10% fetal calf serum, 2 mM glutamine, 1.5 g/liter sodium bicarbonate, 4.5 g/liter glucose, 1 mM sodium pyruvate, 10 mM HEPES, 100 units/ml penicillin, and 0.1 mg/ml streptomycin. When grown in serum-free media, 0.1% BSA was added.

For analysis of c-Kit transphosphorylation, cells were starved in serum-free medium for 12 h and inhibitory or control peptides at the indicated concentrations, or vehicle (0.1% Me₂SO) were added for 1 h. 50 ng/ml human recombinant stem cell factor (SCF, Calbiochem) was added for the last 10 min of incubation. Cells were lysed on ice in lysis buffer B containing 20 mM Tris, pH 7.4, 10% glycerol, 1 mM EDTA, 1 mM EGTA, 0.5% Triton X-100, 0.5 mM sodium orthovanadate, 10 mM β -glycerophosphate, 5 mM sodium pyrophosphate, 50 mM sodium fluoride, and protease inhibitor mixture. The lysates were centrifuged for 20 min at 14,000 rpm, and the supernatants were subjected to SDS-PAGE, and probed with either polyclonal anti-phospho-c-Kit Ab (Cell Signaling Technology) or anti-actin Ab (Sigma) as a marker for total protein.

For NCI-H526 cell proliferation assay, 96-well plates containing eight replicates per assay condition were seeded at a density of 1×10^4 cells in 0.1 ml of serum-free media, and 16 h later the cells were stimulated with SCF (100 ng/ml), and incubation was continued for 72 h. Peptides or vehicle (0.1% Me₂SO) were added 30 min before the addition of SCF. Cell growth was measured using the XTT (Biological

¹ The abbreviations used are: BSA, bovine serum albumin; PBS, phosphate-buffered saline; Abs, antibodies; GST, glutathione S-transferase; mAb, monoclonal antibody; PKB, protein kinase B; GSK, glycogen synthase kinase; SCF, stem cell factor; ERK, extracellular regulated kinase; IGF-1, insulin-like growth factor-1; PKA, protein kinase A; JNK, N-terminal c-Jun kinase; CDK, cyclin-dependent kinase; IRK, insulin receptor kinase; ILK, integrin-linked kinase; Alk-1, activin receptor-like kinase 1; MAPK, mitogen-activated protein kinase.

Industries Bet-Haemek Ltd., Israel) colorimetric dye reduction method. Growth was calculated by subtracting the absorbance at 450 nm of the non-stimulated cells from all systems. The growth of the SCF-stimulated cells was defined as 100% growth, and other systems were expressed relative to it.

Cytosolic FKHR Levels and ERK Phosphorylation in Breast Cancer Cells Treated with PKB-derived Peptide—Breast cancer MDA-MB-231 cells were serum starved and incubated with vehicle (AMI159 formulation, see below), 20 μ M phosphatidylinositol 3'-OH kinase inhibitor LY294002 (Calbiochem), PKB-derived peptide KRX-014_{H151} in AMI159 formulation, or a control peptide derived from Lyn for 18 h. Cells were subsequently stimulated with 50 ng/ml insulin-like growth factor 1 (IGF-1) for 10 min, washed with ice-cold PBS, and lysed in lysis buffer B1 (lysis buffer B containing 1% Triton X-100). Lysates were probed with antibodies against forkhead (Cell Signaling Technology), GSK3 (Transduction Laboratories), phosphorylated-ERK (Sigma), and ERK (Santa Cruz Biotechnology). For AMI159 formulation, peptide (10 mg) was dissolved in 0.4 ml of 0.2% acetic acid and 5% mannitol in TDW and agitated by vortex. 0.15 ml of PG solution (4% benzyl alcohol, 4% pluronic L44, and 2% benzyl benzoate in propylene glycol) was added and vortexed. The solution was heated at 100 °C for 15 min, and neutralized by gradual addition of 0.15 ml of 100 mM phosphate buffer, pH 6.5, and 0.3 ml of 100 mM phosphate buffer, pH 7.0. The solution was spun in a Polytron at 20,000 rpm for 2 min, heated to 100 °C for 15 min, spun again in a Polytron at 20,000 rpm for 2 min, and heated to 100 °C for 30 min.

p27^{Kip1} Levels in Breast Cancer Cells Treated with PKB-derived Peptide—MDA-MB-231 cells grown in Dulbecco's modified Eagle's medium containing 10% fetal calf serum were incubated with vehicle (AK19 formulation, see below), KRX-014_{H151}, or a control peptide at the indicated concentrations for 18 h. Cells were detached using 15 mM EDTA in PBS and resuspended in hypoosmotic buffer containing 10 mM HEPES, pH 7.4, 1.5 mM MgCl₂, 10 mM KCl, 300 mM sucrose, 1 mM EDTA, 0.25 mM EGTA, 0.1% Nonidet P-40, and protease inhibitor mixture. Following centrifugation supernatants were resolved on SDS-PAGE and probed with anti-p27^{Kip1} mAb (Transduction Laboratories) and polyclonal anti-actin Ab (Sigma). AK19 formulation was 5 mg/ml peptide in 0.2% acetic acid, 1% pluronic L44, and 5% mannitol neutralized with 0.3 M sodium bicarbonate.

PKB Phosphorylation in Prostate Cancer Cells Treated with PDK1-derived Peptide—Prostate cancer DU-145 cells were serum-starved for 14 h and exposed to vehicle (0.1% Me₂SO) or peptides at the indicated concentrations for the last 4 h of starvation. Cells were stimulated with IGF-1 (50 ng/ml) for 10 min and lysed with lysis buffer B1. Equal amounts of protein were separated on SDS-PAGE, and probed with anti-phospho-PKB(T308), anti-phospho-PKB(S473), both from Cell Signaling, and anti-GSK3 Abs.

Aortic Ring Assay—All animal procedures were approved by the animal care and use committee of the Hebrew University. As previously reported (26), thoracic aortas were dissected from 8–10-week-old male BALB/c mice. The aortas were immediately transferred to Petri dishes containing BIO-MPM-1 (Biological Industries Ltd., Israel). The adventitia and small vessels around the aorta were carefully removed under a dissecting microscope, and transverse cuts of 0.5 mm were made. The resulting aortic rings were extensively rinsed and incubated overnight in BIO-MPM-1 containing penicillin-streptomycin. Subsequently, the rings were embedded in 600–800 μ l of a collagen mixture (7 parts rat tail collagen (27), 1 part \times 10 minimal essential medium (biological industries), and 2 parts 0.15 M sodium bicarbonate) in 24-well plates. Raising the pH to neutral and the temperature to 37 °C achieved solidification of the collagen solution. In each well, 3 aortic rings were embedded. Medium (400 μ l of Endo-SFM (Invitrogen) containing penicillin-streptomycin and 30 ng/ml SCF with 10 μ M peptide or vehicle were added to the embedded rings, and the plates were incubated at 37 °C in a humidified 10% CO₂ atmosphere. Medium containing SCF and either peptides or vehicle was replaced 3 times a week. After 7 days, the rings were fixed with 4% formaldehyde for 24 h, followed by staining with crystal violet (0.02%) dissolved in ethanol, and extensive washing to remove excessive stain. The effect of SCF and peptides was examined in 3 wells (9 rings) per peptide. Micrographs of representative rings were taken using a digital camera (Nikon, Japan). Morphometric analysis of sprouting was performed manually using Image-Pro 4.5 software (MediaCybernetics) according to Nissanov *et al.* (28).

RESULTS

KinAceTM Regions: Definition, Patterns, and Analysis of Three-dimensional Structures and Mutational Data—The

KinAceTM platform targets well defined regions, consisting of subdomain V (the α D region), the loop between subdomains IX and X (named the HJ loop (24), known also as L13 (19, 24), and the subdomain X (the α G helix) of the catalytic domain of the kinase (Fig. 1a; subdomain definitions follow Hardie and Hanks (29)). The KinAceTM regions are common to all protein kinases and share characteristic structural patterns, detailed below. We analyzed kinase-substrate interactions in all kinase-substrate, kinase-pseudosubstrate, and kinase-autoinhibitory structures solved to date with <2.8 -Å resolution. In addition, we searched the literature for mutational data elucidating the role of residues in these regions. The following is a detailed account of each of the KinAceTM regions.

The HJ- α G region (subdomains IX-X of the kinase catalytic domain) corresponds to residues ²³⁰EMAAGYPPFFADQPI-QIYEKIV²⁵¹ in cAMP-dependent protein kinase (PKA), and is shown as a *red ribbon* in Fig. 1a. The three-dimensional framework is common to all protein kinase structures solved so far, as illustrated in Fig. 1b. Sequence and structural alignment of residues in this region from various kinases, reveals a characteristic template. The template consists of a short conserved helix (positions 1–3), a variable strand around a conserved glycine at position 6, a conserved hydrophobic PF or PY dip (positions 9–10) buried in the protein structure, a variable shoulder-like region (positions 11–15), followed by a variable helix (positions 16–22), which is anchored to the protein by two conserved hydrophobic residues (positions 18 and 22). The conserved residues are *boxed in blue* in Fig. 1d.

Highly variable patches interspace the typical sequence pattern of conserved residues as shown in Fig. 1d. Interestingly, conserved regions are buried, whereas the variable spacers are exposed to the solvent and thus available for binding (Fig. 1c). Variability may be responsible for specific recognition of the kinase-binding partners.

Several crystallographic (22, 23, 39, 43, 45) and mutational (26, 31, 35) studies have pointed to HJ- α G residues as being involved in substrate binding and in binding to upstream activators (36). A careful analysis of all crystal structures of kinases complexed with peptidic substrates (30–36), pseudosubstrate (37), or autoinhibitory units docked in the substrate binding groove (22, 45, 48) reveals that the HJ- α G region is involved in interactions with the substrates in all the structures except in the phosphorylase kinase (PHK) complex (30), probably because of the shortness of the substrate peptide (Fig. 1d and Supplemental Materials Appendix A). Seven to 10 amino acids before and after the PF dip typically participate in substrate binding and in some cases were shown to determine selectivity toward substrate (20, 39, 40). These patches fall within the exposed and variable parts of the HJ- α G template that we proposed as substrate binding determinants. The conserved and buried dip (positions 9–10) and the anchors (positions 18 and 22) do not bind the substrate but may rather serve as a structural scaffold that enables the surrounding variable residues to present themselves to the substrate.

The α D region throughout this work refers to residues corresponding to ¹²³VAGGEMFSLRRIGRFSE¹⁴¹ in PKA (positions 1–19), shown as a *blue ribbon* in Fig. 1a. The α D role in substrate binding was discussed in several structural works (21, 31, 35, 41). We have supplemented these findings by highlighting substrate-neighboring residues in kinase-substrate (30–32, 34), -pseudosubstrate (37, 42), or -autoinhibitory substrate-like peptide (21, 43–46) complexes published so far. We found that in 90% of the structures the α D residues are in close contact with or hydrogen bonded to the substrate. Site-directed mutagenesis (20, 40, 47–50) and naturally occurring mutations (51, 52) in this region were shown to affect the kinase function

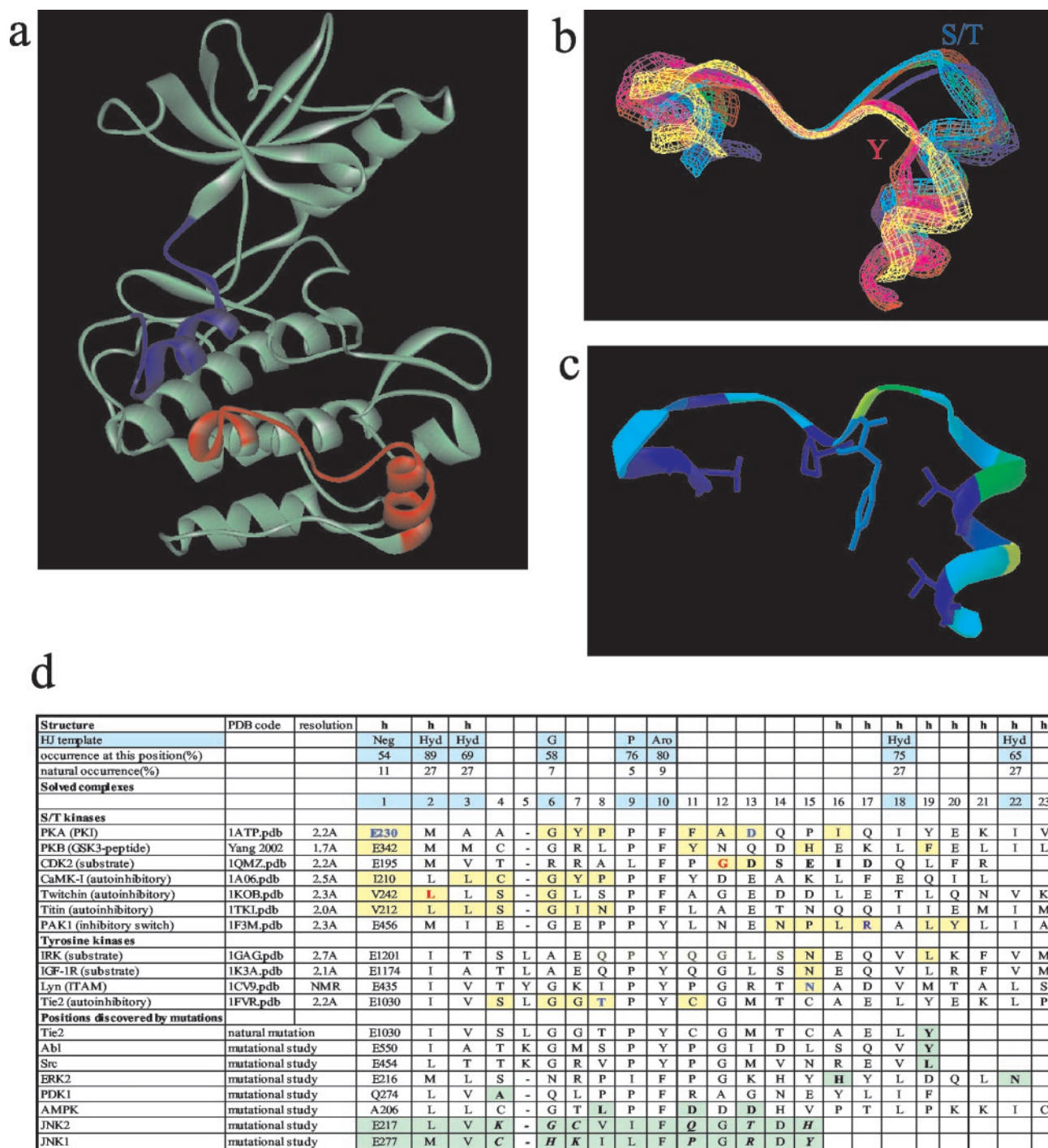


FIG. 1. HJ- α G region participates in substrate binding. *a*, PKA (Protein Data Bank code 1ATP) is depicted in ribbon representation with α D and HJ- α G regions colored blue and red, respectively. The picture was prepared with ActiveX freeware (accelrys.com). *b*, ribbon representation of HJ- α G regions of the Ser/Thr kinases twitchin (depicted in lilac, Protein Data Bank code 1KOB), phosphorylase kinase (green, Protein Data Bank code 2PHK), PKA (red, Protein Data Bank code 1ATP), CaMK-I (blue, Protein Data Bank code 1A06), titin (cyan, Protein Data Bank code 1TKI), p21-activated kinase 1 (PAK1) (yellow, Protein Data Bank code 1F3M), and the tyrosine kinases IRK (red, Protein Data Bank code 1GAG), IGF-1R (purple, Protein Data Bank code 1K3A), and Tie2 (magenta, Protein Data Bank code 1K3A). The kinases were superimposed using "Fit selected residues" option in Swiss-PdbViewer, using the selected residues that correspond to Pro²³⁶-Pro²³⁷-Phe²³⁸ in the Protein Data Bank code 1ATP structure of PKA. *c*, HJ- α G region of IRK (Protein Data Bank code 1IRK) is depicted in ribbon representation, colored by accessibility using Swiss-PdbViewer freeware (swissmodel.unibas.ch). The colors vary from the buried blue to the accessible yellow. The side chains of the conserved residues Glu¹²⁰¹, Pro¹²⁰⁹, Tyr¹²¹⁰, Val¹²¹⁸, and Val¹²²² are shown. These residues are buried into the protein, and are spaced by variable, solvent accessible residues, whose side chains are not shown in this figure. *d*, the HJ- α G region has a characteristic well conserved three-dimensional framework common to all kinases. HJ- α G residues involved in substrate or pseudosubstrate binding as found in the Protein Data Bank structures and in published mutational studies. The structural motif of the region, named the HJ- α G template, is marked by blue background, *h* stands for helix, occurrence (%) of the conserved among 55 kinases compiled and aligned by Hardie and Hanks (29) is written below compared with normal frequency. The occurrences of individual amino acids were taken from Jones *et al.* (38). *Hyd* stands for the hydrophobic Leu, Met, Ile, Val, and Phe residues; *Pos* for the positively charged Lys, Arg, and *His* and *Neg* for the negatively charged Asp and Glu; G and P are glycine and proline, respectively. The sequences are aligned, and the number of the first residue is written for easier referencing. Residues that are found within 4.0 Å of the substrate or pseudosubstrate are boxed in yellow background. When a side chain of the HJ region residue makes hydrogen bond with the substrate or the pseudosubstrate the residue is written in blue. When the backbone makes the hydrogen bond, the residue is written in red. Where the importance of the residue for downstream signaling or substrate phosphorylation was shown by mutational studies or naturally occurring mutations, it is depicted on a green background. Residues that significantly differ between JNK1 and JNK2 are written in italics.

α D pattern	region	peptide sequence																											
c-Kit KRX-147 _{D103}	α D	Myr	G				N	L	L	N	F	L	R	R	K						NH ₂								
Lyn KRX-055 _{G106}	HJ- α G	Myr	G															R	T	N	A	N	V	<i>Nle</i>		NH ₂			
PDK1 KRX-702 _{H105}	HJ- α G	Myr	G	G														R	A	G	N	<i>Q</i>	Y	L		NH ₂			
PKB KRX-014 _{H151}	HJ- α G	Myr	G	G														Y	N	<i>Q</i>	N	H	<i>Q</i>	K	L	F	<i>Q</i>	L	NH ₂
PDK1 KRX-702 _{D103}	α D	Myr	G		G	<i>Q</i>	L	L	K	Y	I	R														NH ₂			
ERK KRX-137 _{D103}	α D	Myr	G		G	N	L	Y	K	L	L	K														NH ₂			
c-Kit KRX-147 _{H101}	HJ- α G	Myr	G				S	L	G	S	S	P	Y	P												NH ₂			
Lyn KRX-055 _{H235}	HJ- α G	Myr	G											Y	P	G	R	T	N	A	N	V	M	T		NH ₂			
PDK1 KRX-702 _{H103}	HJ- α G	Myr	G				G	G	L	P	P	F	R	A	G											NH ₂			
ERK KRX-137 _{H103}	HJ- α G	Myr	G				G	R	P	I	F	P	G	K	Y											NH ₂			
HJ- α G pattern								G				P	Y													Hyd			

FIG. 3. **Peptide sequences.** Summary of peptides used in this study. The active peptides for each of the systems of interest are boxed in gray; the rest of the peptides were used for control. All peptides are *N*-modified by myristoyl-glycine (Myr-G). *Nle* stands for norleucine. Substitutions of negatively charged residues by neutral analogs are shown in italics. The peptides are aligned to HJ- α G and α D conserved templates.

substrate binding by tyrosine kinases is further supported by mutational studies of IRK (51, 52) and Abl (40) as well as structural analysis of Tie2 (46). Fig. 2*b* shows that these residues overlay well between different kinases, and create a characteristic structural motif for substrate binding. In Ser/Thr kinases the triad of positions 5, 7, and 11 extends toward the substrate and is involved in substrate binding, as demonstrated in PKA/PKI structure (Fig. 2*c*). It is interesting to note that the least conserved positions 7 and 11 are important both for binding of Ser/Thr kinase substrates and of tyrosine kinase substrates. This variability may contribute to specificity of the kinase in substrate recognition. α D residues that occupy the side of the helix that is opposite the substrate binding region were found to participate in binding an inhibitory protein by Cdk6 (53) and to be part of a docking groove of MAPK interacting proteins (54) (Supplemental Materials Appendix B and Fig. 2*a*).

KinAceTM Peptide Inhibitors—We have systematically derived series of peptides of 6 to 14 amino acids in length from both subdomains V and X–XI of several protein kinases of interest. The peptides span the entire KinAce regions and partially overlap. Based on the analysis presented above, residues that are solvent exposed, hypervariable, or were pointed out to be involved in substrate binding by mutational or structural studies, were considered as potential binding sites. Each peptide was designed to include several such residues.

The peptides derived from the HJ- α G domain could be clustered in three groups: subregion I (positions 2–8), subregion II (the residues surrounding the PF dip, positions 7–13), and subregion III, corresponding to the exposed and variable shoulder and the α G helix (positions 11–23). We derived an average of 20 peptides per kinase that were initially screened in cell-based assays. These assays provide intact substrate in its native form, which is crucial in cases where the inhibitor is derived from the kinase and is therefore expected to bind the substrate. Moreover, the cell-based assays expose the peptide inhibitor to the entire set of the kinase substrates. When a substrate of the kinase of interest is well defined in the relevant cell line, the peptides were screened for inhibition of the kinase activity on that substrate in the cell. For kinases involved in proliferative diseases, cell growth assays were performed, providing the net effect of the peptide on cell survival. This straightforward test is particularly advantageous when the relevant substrates of the kinase are not known.

Fifteen to 30 peptides were derived from the tyrosine kinases c-Kit and Lyn, and the Ser/Thr kinases PDK1 and PKB. On average, one-third of the peptides, from HJ- α G, α D, or both

regions, were found active. Most of the active HJ- α G peptides belong to subregion III, others to subregion I, and almost none to subregion II. Here we present the results for a representative active peptide for each of the kinases.

The derived peptides were *N*-myristoylated and C-amidated to enhance cell permeability and metabolic stability (55–58). We have previously shown that *N*-myristoylated C-amidated peptides penetrate the cell membrane (24, 25). Negatively charged residues (aspartate and glutamate) were usually modified to their neutral analogs (asparagine and glutamine, respectively) to further improve cell permeability (59, 60). The sequences of the active peptides (boxed in gray) and the control peptides used in the biochemical assays are listed in Fig. 3 and are aligned according to the HJ- α G or α D templates.

Molecular and Cellular Characterization of a c-Kit-derived Peptide—SCF receptor is a proto-oncogene, which belongs to the type III receptor tyrosine kinase subfamily (61). SCF engagement of the c-Kit extracellular binding domain leads to receptor dimerization, followed by intracellular transphosphorylation of tyrosine residues (62, 63). This, in turn, creates specific docking sites for a broad set of signal transduction molecules and induces substrate binding and phosphorylation (64, 65). SCF and c-Kit were shown to be critical for the survival and development of stem cells involved in hematopoiesis, melanogenesis, and fertility.

Three peptides, covering the HJ- α G region were derived and found inactive. Ten peptides, covering positions 5–17, were derived from the α D region. Seven of these peptides were found active. Substitution of the aspartate subsequent to the myristoyl-G moiety was found necessary for peptide activity. Moreover, the presence of either binding determinants 7 and 11 or binding determinants 11 and 14 is essential for activity. In peptides spanning positions 5–13 and lacking binding position 14, deletion or substitution of the positive residues at positions 12 and 13 abrogated peptide activity. This data suggests that the positive charge at positions 12 and 13 might compensate for the lack of positively charged binding determinant 14. A representative active peptide that spans positions 5–13, KRX-147_{D103} was chosen for further analysis.

To test KRX-147_{D103} activity, c-Kit-expressing NCI-H526 small cell lung cancer cells were incubated with various concentrations of the c-Kit-derived peptide KRX-147_{D103} and control peptides derived from Lyn (KRX-055_{G106}), PDK1 (KRX-702_{H105}), or from the HJ- α G region of c-Kit (KRX-147_{H101}). Fig. 4*a* demonstrates that KRX-147_{D103} selectively inhibited c-Kit transphosphorylation, induced by SCF, with an IC₅₀ value of 7 μ M, whereas no inhibition was detected with any of the control

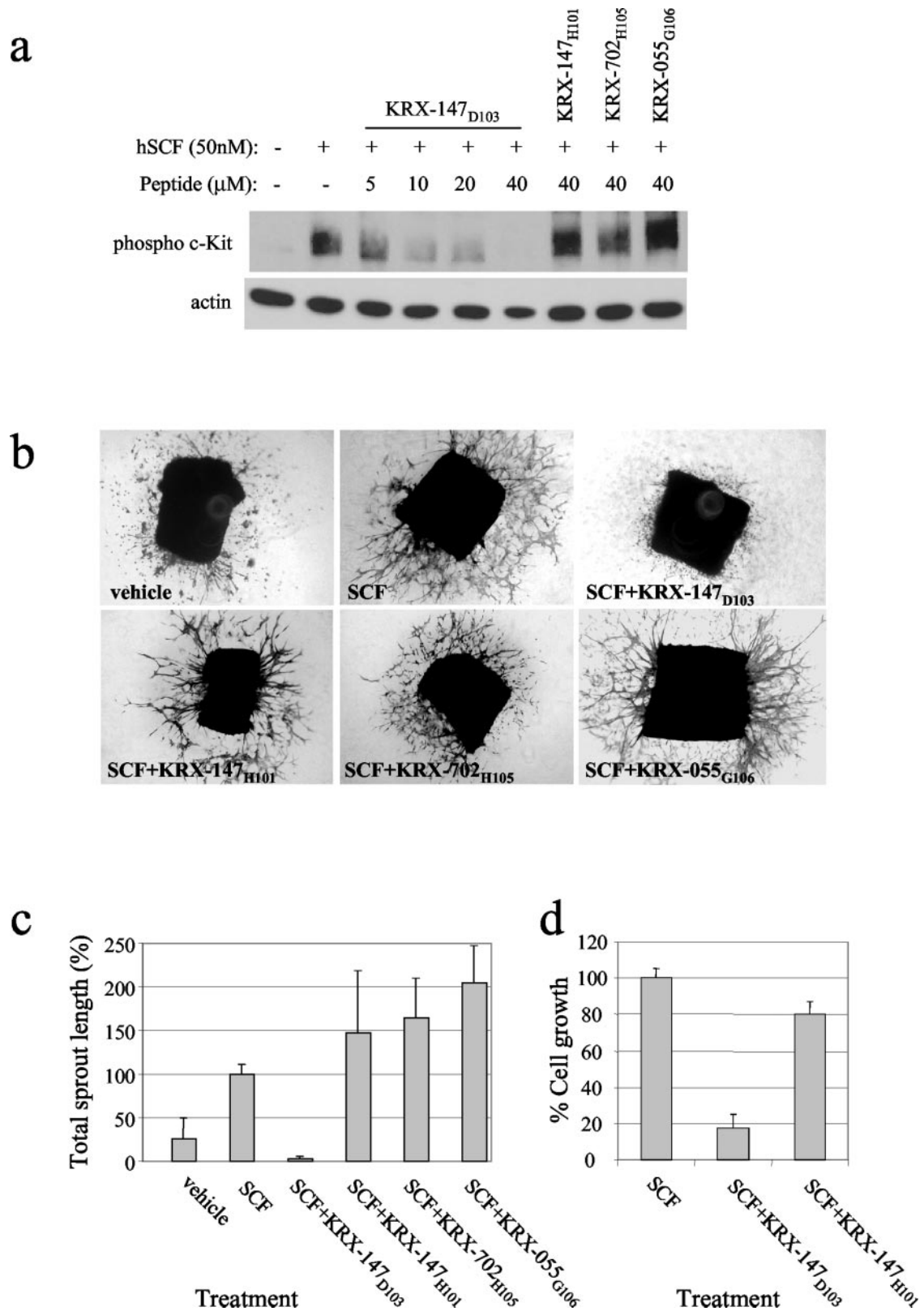


FIG. 4. **a** c-Kit derived peptide KRX-147_{D103} inhibits c-Kit autophosphorylation, aortic ring sprouting, and SCF-induced growth of c-Kit expressing cells. *a*, small cell lung cancer cells, NCI-H526, were serum-starved for 12 h. Preincubation of the cells with the peptides for 1 h at the indicated concentrations was followed by 10 min stimulation with human recombinant SCF. Samples were subjected to Western blotting with anti-phospho-c-Kit Ab and protein levels were visualized using anti-actin Ab. The autoradiogram is representative of three experiments. *b*, aorta of BALB/c mice was cleaned and cut to transverse sections of 0.5 mm. Rings were embedded in collagen matrix and were exposed for 7 days to 30 ng/ml of mouse recombinant SCF and either vehicle (0.1% Me₂SO) or 10 μ M peptides. Rings were fixed and stained with 0.02% crystal violet to illustrate sprouting. A representative micrograph of each arm of the experiment is shown. *c*, statistical morphometric analysis of sprout length. Four repeats of each treatment were measured, and mean \pm S.E. is presented relative to the rings treated with SCF. *d*, NCI-H526 cells were grown in serum-free media overnight, and then stimulated with SCF (100 ng/ml). Peptides at 10 μ M concentration were added 30 min before the addition of SCF. Cell growth was measured using the XTT colorimetric dye reduction method, 72 h after the addition of growth factor. Data are representative of two independent experiments.

peptides even at 40 μM concentration. Testing the inhibitory effect of the peptides on SCF-induced proliferation of NCI-H526 cells, we show that the αD -derived KRX-147_{D103} inhibited cell growth, whereas the HJ-derived KRX-147_{H101} had only a minor effect (Fig. 4d), in accordance with the rest of our data.

The involvement of c-Kit ligand SCF in angiogenesis was reported by Zhang and co-workers (66). Angiogenesis is a complex intercellular process that involves proliferation, migration, and organization of various cells. We thus tested the anti-angiogenic activity of the peptide on sprouting of mouse aortic rings in an *ex vivo* assay. Fig. 4, b and c, demonstrates that at 10 μM , KRX-147_{D103} totally blocked SCF-induced vessel formation, whereas no inhibitory effect was detected using control peptides at the same concentration.

Molecular and Cellular Characterization of a PDK1-derived Peptide—PDK1 is a Ser/Thr kinase that selectively phosphorylates Thr-308 on the activation loop of PKB, thereby boosting PKB activity by at least 100-fold (67). This kinase mediates multiple signaling pathways that are coupled to growth factor receptor activation, especially in human cancers. PDK1 is highly expressed in the majority of human breast cancer cell lines and its activation was suggested to be involved in mammary tumorigenesis (68). Targeting PDK1 was put forward as a novel therapeutic approach for diseases such as diabetes and cancer (67, 69).

Fourteen peptides were derived from the entire KinAceTM regions of PDK1, 10 from the three HJ- αG subregions and 4 from the αD region. The peptides were screened for their ability to inhibit the phosphorylation of the well defined direct substrate of PDK1, PKB(T308), in intact cells and to inhibit prostate cancer cell proliferation. Four peptides were found active. Three of them were derived from the variable and solvent exposed, shoulder-like subregion III of the HJ- αG domain and one from αD (positions 7–11). The most potent lead, KRX-702_{H105}, spans positions 11–17 of subregion III of the HJ- αG (Fig. 3). This region was implicated in binding of substrates by most of the kinases listed in Fig. 1d (detailed in Supplemental Materials Appendix A).

Fig. 5a shows that KRX-702_{H105} inhibited the phosphorylation of PKB(T308) in IGF-1 stimulated prostate cancer DU-145 cells in a dose-dependent manner, whereas no inhibition was observed with KRX-702_{H103}, a control peptide derived from subregion II of PDK1 (Fig. 3). In addition, selectivity is demonstrated by the finding that KRX-702_{H105} had only a minor effect on the phosphorylation of PKB(S473) (Fig. 5a). Moreover, the peptide had no effect on c-Kit activity as mentioned above (Fig. 4).

Because PDK1 is involved in signaling pathways that regulate cell growth and survival, KRX-702_{H105} was tested in a cell proliferation assay. The hormone refractory prostate cancer PC3 cells possess high levels of activated PKB because of deletion in its negative regulator PTEN, and therefore their viability is expected to be PKB-dependent (70, 71). The peptide at 10 μM concentration inhibited the growth of PC3 cells by 40% as compared with the vehicle control (Fig. 5b). This moderate inhibition may be because of the fact that KRX-702_{H105} had almost no effect on the phosphorylation of Ser-473 and therefore a partial PKB activity was retained (72). No effect on PC3 cell proliferation was observed using the control peptide KRX-702_{H103}.

Molecular and Cellular Characterization of a PKB-derived Peptide—A wide variety of studies have implicated the Ser/Thr kinase Akt/PKB in cell transformation through inhibition of apoptosis, growth stimulation, and regulation of metabolic processes (reviewed in Ref. 73). Dysregulation of PKB has been

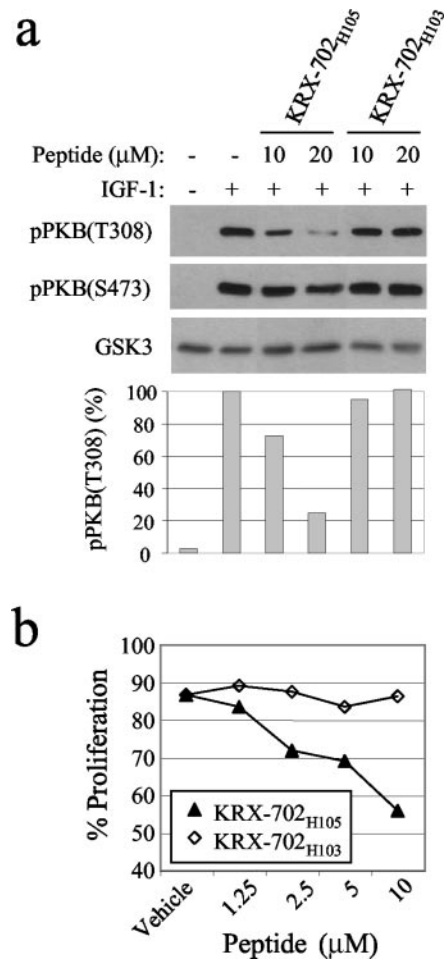


FIG. 5. A PDK1-derived peptide KRX-702_{H105} specifically inhibits the phosphorylation of PKB(T308) in prostate cancer cells and inhibits cell growth. *a*, DU-145 cells were starved for 14 h and exposed to the vehicle (0.1% Me₂SO, marked as -) or peptides at the indicated concentrations for the last 4 h of starvation, prior to 10 min stimulation with IGF-1. Samples of 25 μg of protein were separated on SDS-PAGE and probed with anti-phospho-PKB(T308) Ab and anti-phospho-PKB(S473) Ab to detect PKB phosphorylation, and anti-GSK3 Ab to verify equal amounts of protein loaded. Histograms represent the levels of phosphorylated PKB(T308) in each treatment relative to cells activated by IGF-1 in the presence of the vehicle. The autoradiogram is representative of four independent experiments. *b*, prostate cancer PC3 cells were exposed to various concentrations of KRX-702_{H105} in the formulation (\blacktriangle) for 72 h and cell number was measured by the methylene blue method. KRX-702_{H103} (\diamond) was used for control. For more details see “Experimental Procedures.”

associated either as a primary or secondary etiologic factor in many neoplastic processes. The viral oncogene, v-Akt, is associated with the murine leukemia virus AKT8, and overexpressed PKB has been found in prostate, pancreatic, ovarian, breast, and gastric tumors in humans, and is associated with poor prognosis (74–76). Overactivation of PKB has been associated with inactivating mutations of PTEN, a tumor suppressor phosphatase that ordinarily down-regulates the activity of PKB (77). Inactivating mutations in PTEN exist in 60% of all forms of solid tumors. Thus, modulation of the PKB signaling pathway is an excellent target for kinase-based therapeutic interventions.

Ten of 30 PKB-derived peptides were found active. Most of the active peptides were derived from the accessible and variable shoulder (subregion III) of the HJ- αG region of PKB, and KRX-014_{H151} (Fig. 3) was chosen as a representative. The Tyr, His, and Phe residues in this peptide have been suggested as important pharmacophors for substrate binding based on a

crystal structure recently solved by Yang and co-workers (31) (Fig. 1*d*).

In a cell-free kinase assay KRX-014_{H151} inhibited the phosphorylation of the PKB substrate GSK3 by PKB. At the same concentrations, control peptides derived from Lyn, PDK1, or ERK had no inhibitory effect (Fig. 6*a*). Because GSK3 serves as a substrate for several other kinases in intact cells, we chose to test a more exclusive PKB-dependent signaling, the forkhead-p27^{Kip1} pathway.

Treatment of cells with many growth factors, such as IGF-1 (78), platelet-derived growth factor (79), or epidermal growth factor (80), leads to activation of PKB, which subsequently phosphorylates forkhead transcription factors. This phosphorylation results in nuclear exclusion of the forkhead family members (81, 82) and consequent inhibition of p27^{Kip1} expression (83). The effects of KRX-014_{H151} on breast cancer MDA-MB-231 cytosolic levels of FKHR (also called FOXO1), and on p27^{Kip1} expression levels are presented in Fig. 6, *b* and *c*, respectively. It is apparent that following treatment with KRX-014_{H151}, the cytosolic levels of FKHR are reduced, whereas the levels of p27^{Kip1} are elevated. These effects are consistent with inhibition of PKB phosphorylation of FKHR. The control peptides in these assays, derived from Lyn kinase, do not show similar effects (Fig. 6, *b* and *c*). We have further tested the selectivity of this PKB-derived inhibitor and demonstrated that KRX-014_{H151} does not inhibit the ERK pathway, another main signaling pathway stimulated by IGF-1 (Fig. 6*d*).

Because PKB is an anti-apoptotic enzyme, which plays a pivotal role in cell survival and growth, we examined the effect of the PKB-derived peptide on breast cancer MDA-MB-231 cell proliferation. Incubation of these cells with KRX-014_{H151} for 3 days resulted in 90% inhibition in the presence of 10 μM peptide and with an IC₅₀ value of 3 μM (Fig. 6*e*). The proliferation of MDA-MB-231 cells was not affected by the control peptide KRX-055_{H235} (Fig. 6*e*), shown to be inactive in the PKB activity assay in cells (Fig. 6*b*).

Molecular Characterization of a Lyn-derived Peptide—The Src-related protein kinase Lyn was originally discovered in the context of hematopoietic cells, where it plays a role in the regulation of B cell immune responses (84). Evidence presented by others (85–87) and by our group indicates that Lyn is also involved in the control of development and proliferation of the prostatic epithelium. We have previously found that a short peptide, derived from subregion I of the HJ- α G domain of Lyn kinase: (i) inhibits Lyn kinase activity in a cell-free assay, (ii) inhibits Lyn transphosphorylation and interferes with Lyn-dependent signaling in intact B cells; (iii) inhibits the proliferation of Lyn-expressing HRPC cells; and (iv) induces regression of tumors following injection to mice bearing HRPC xenografts (24).

We have derived 30 peptides from Lyn KinAceTM regions. Seven peptides were found active, most of them from subregion III and some from subregion I of the HJ- α G domain. In this study we present a subregion III derived active peptide, KRX-055_{G106} (Fig. 3). The native Met⁴⁵³ (see Fig. 1*d* for numbering of residues) was substituted to norleucine to avoid oxidation of the native methionine (88). The peptide includes Asn⁴⁴⁹ that potentially forms a hydrogen bond with the Lyn substrate in the Lyn-immunoreceptor tyrosine-based activation motif complex (36). Furthermore, two unique residues may serve as specificity determinants for substrate recognition based on Src family sequence alignment: Arg⁴⁴⁷ at position 13, which is populated by methionine in the rest of the Src family members, and Ala⁴⁵⁰ at position 16 that is unique within the Src family for Lyn and Fyn-related kinase only. Position 13 was found important for substrate binding by mutational studies of

AMPK (20) and JNK (39). Furthermore, this position participates in substrate binding in the kinase-substrate complexes of CDK2 (32) and PKA (37).

We demonstrated the activity and selectivity of the Lyn-derived peptide using cell-free kinase assays. To that end we have cloned, expressed in bacteria, and purified two intact proteins known as Lyn substrates: non-phosphorylated Lyn, which can be transphosphorylated by active Lyn (89), and Syk, which is a well known Lyn substrate in B cells (90). In Fig. 7, *a* and *b*, we show that while KRX-055_{G106} potently inhibits the phosphorylation of Syk and Lyn in a dose-dependent manner, yielding 90 and 80% inhibition at 5 μM concentration, respectively, no inhibition was detected with control peptides derived from ERK, PDK1, or c-Kit, at the same concentration. Selectivity was further examined against another member of the Src family, the tyrosine kinase Src. As mentioned above, KRX-055_{G106} contains two unique residues, as compared with Src, that may affect substrate recognition (marked in bold at the bottom of Fig. 7*c*). KRX-055_{G106} had no inhibitory effect on Src transphosphorylation at 5 μM concentration and only a minor effect was detected at higher concentrations (Fig. 7*c*). Likewise, KRX-055_{G106} had no inhibitory effect on an additional tyrosine kinase, c-Kit (Fig. 4).

The involvement of Lyn in HRPC cell survival and growth was recently discovered, as mentioned above. We therefore examined whether KRX-055_{G106} affects DU-145 cell proliferation, and show that the growth of DU-145 cells was potently inhibited by the peptide at IC₅₀ value of 1.5 μM (Fig. 7*d*). Control peptides from ERK, PDK1, or c-Kit, which had no effect on Lyn activity in kinase assay, were found inactive in cell proliferation assays as well. A control peptide, KRX-055_{H213} derived from Lyn subregion I, but lacks a main pharmacophore because of substitution to alanine, was found inactive in both assays of kinase activity (data not shown) and cell proliferation (Fig. 7*d*).

KinScreen Technology—We have exemplified the potential of the KinAceTM technology to generate selective inhibitors for kinases, using cell-free and intact cell assays. The KinScreen technology utilizes this aptitude to identify the involvement of a specific kinase in a selected disease. Taking cancer as a disease of interest, a cell proliferation assay is used to test the contribution of various kinases to the growth of cancerous cell lines. The contribution of the kinase is examined by measuring the inhibitory effect of the peptides derived from the KinAceTM regions of the kinase. Thus, inhibition of cell proliferation by a certain peptide indicates a potential connection between the kinase from which the peptide was derived and the tumorigenic cell line.

In Fig. 8 we exemplify an array of KinScreen aiming to detect target kinases for oncological indications. Ten myristoylated peptides from eight kinases were derived and tested at concentrations up to 10 μM in a cell proliferation assay of hormone refractory prostate cancer (DU-145 and PC-3), estrogen receptor positive breast cancer (MCF-7), estrogen receptor-deficient breast cancer (MDA-MB-231), colon cancer (HT-29), and ovarian cancer (A2780) cell lines. The inhibitory effect is indicated as percent of survival at 10 μM peptide concentration, only when less than 60% survival was detected.

The peptides tested in this assay were derived from the tyrosine kinases c-Kit, Lyn, Fyn, and Zap-70 and the Ser/Thr kinases Activin receptor-like kinase-1 (Alk-1), integrin-linked kinase (ILK), PKB, and PDK1. In Fig. 8 the KinScreen matrix exposed a novel finding implicating Lyn as a target for hormone-resistant prostate and breast cancers. The Src-related tyrosine kinase Lyn was well characterized as a pivotal player

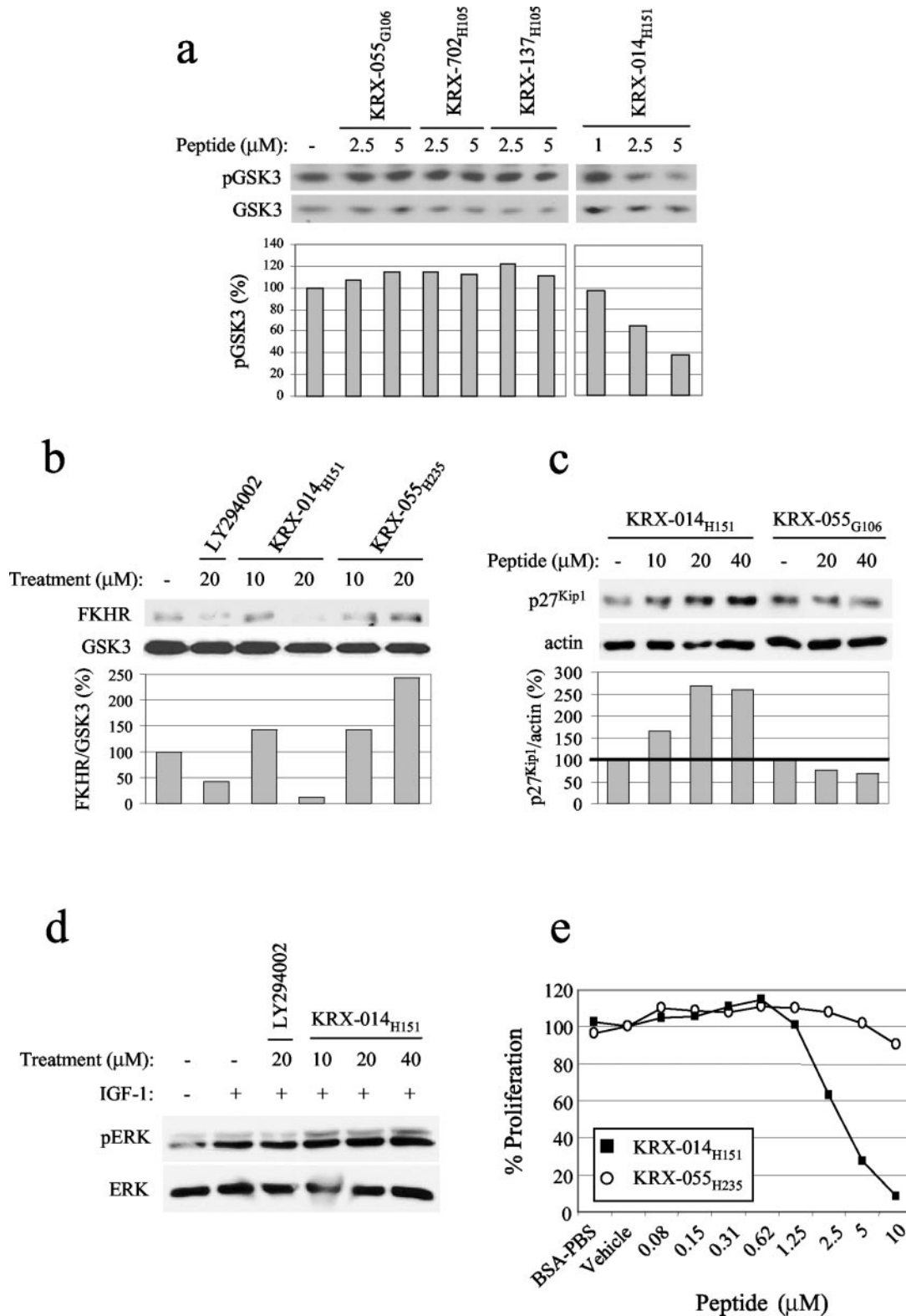


FIG. 6. A PKB-derived peptide KRX-014_{H151} inhibits PKB in a cell-free kinase assay, PKB-dependent signaling in breast cancer cells and leads to growth inhibition. *a*, equal amounts of GSK3, immunoprecipitated from starved DU-145 cells, were incubated with 120 ng/sample of active PKB and the indicated concentrations of KRX-014_{H151}, vehicle (-), or control peptides derived from Lyn, PDK1 and ERK. Following addition of 100 μM ATP and 5 min agitation at 30 °C reactions were stopped by addition of SDS sample buffer, separated on SDS-PAGE, and immunoblotted with anti-phospho-GSK3 Ab (*pGSK3*) followed by reprobing with anti-GSK3 Ab (*GSK3*). *b*, MDA-MB-231 cells were serum-starved and incubated for 18 h in the presence of the vehicle (-), 20 μM LY294002, or KRX-014_{H151} and control peptide derived from Lyn at 10 and 20 μM concentrations. Following stimulation with 50 ng/ml IGF-1 for 10 min, cells were lysed and resolved by SDS-PAGE. Membrane was probed with anti-FKHR Ab or anti-GSK3 Ab. Histograms represent FKHR levels divided by GSK3 levels of each treatment, relative to cells treated with the vehicle. *c*, MDA-MB-231 cells were incubated with the vehicle (-), KRX-014_{H151}, or control peptide derived from Lyn at the indicated concentrations for 18 h. Lysates were resolved on SDS-PAGE, and the membrane was probed with anti-p27^{Kip1} or anti-actin Abs. Histograms represent p27^{Kip1} levels divided by actin levels of each treatment, relative to cells treated with the vehicle. *d*, cells were treated as described in *b* and lysates were probed with anti-phospho-ERK Ab (*pERK*) and reprobed with anti-ERK Ab. *e*, MDA-MB-231 cells were exposed to various concentrations of KRX-014_{H151} (■) or the control peptide KRX-055_{H235} (○) for 72 h, and cell number was determined by methylene blue staining.

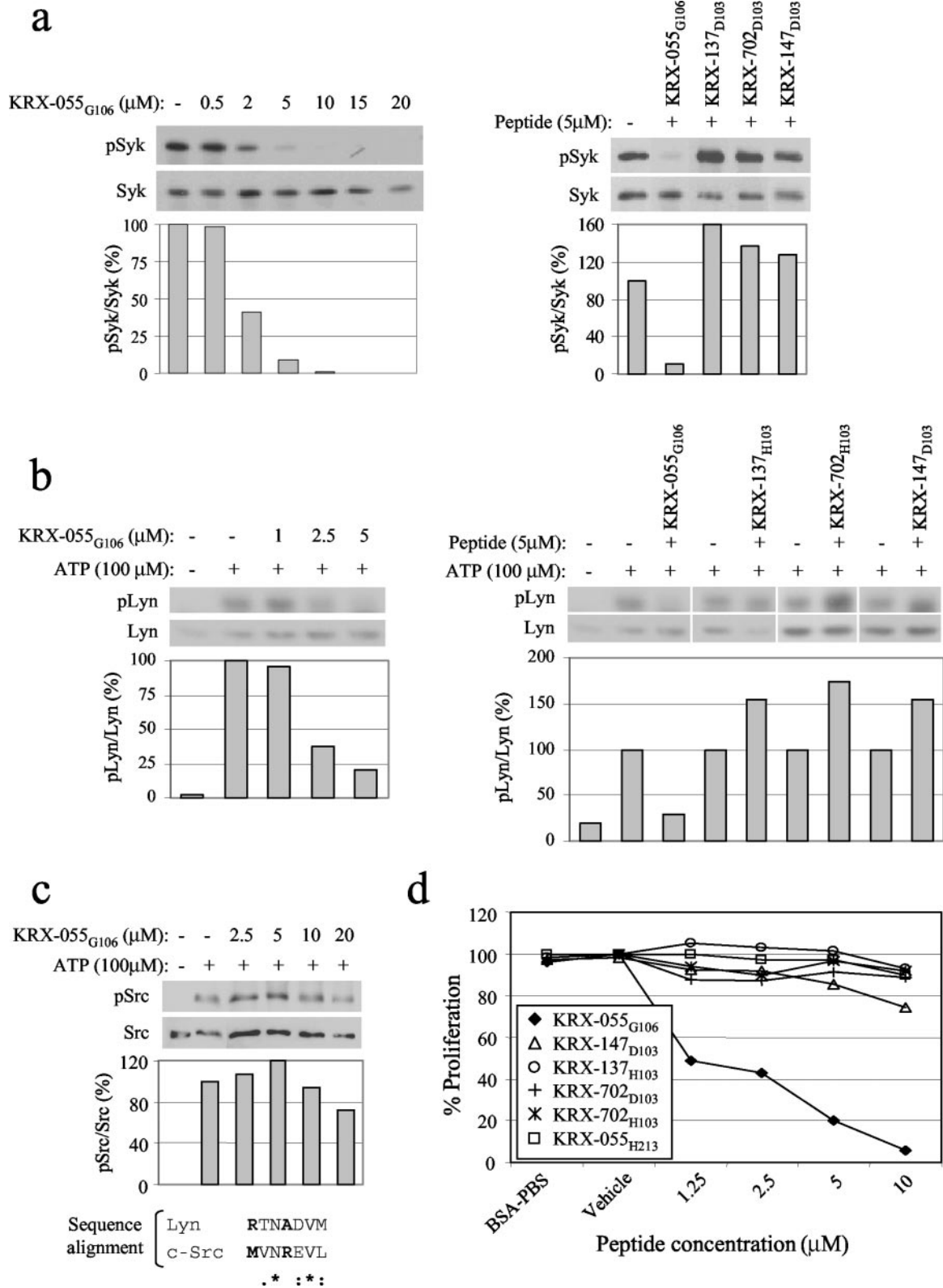


FIG. 7. A Lyn-derived peptide KRX-055_{G106} selectively inhibits Lyn-dependent phosphorylation in cell-free kinase assays and inhibits prostate cancer cell proliferation. Active Lyn was used to phosphorylate either GST-Syk (*a*) or kinase-dead Lyn-K275L (*b*). Samples containing vehicle (1% Me₂SO, marked as -), the indicated concentrations of KRX-055_{G106} (*a* and *b*, left panels), or 5 μM KRX-055_{G106} or control peptides derived from ERK, PDK1, or c-Kit (*a* and *b*, right panels), were incubated with active human Lyn and either GST-Syk (*a*) or Lyn-K275L (*b*). Following addition of 100 μM ATP and agitation at 30 °C for 10 min, reactions were stopped and resolved on SDS-PAGE. Membranes were immunoblotted with anti-Tyr(P) mAb (pSyk in *a* and pLyn in *b*) and reprobbed with anti-Syk Ab (*a*) or anti-Lyn Ab (*b*). *c*, equal amounts of active Src were incubated with either the vehicle (-) or the indicated concentrations of KRX-055_{G106}. Following addition of 100 μM ATP and agitation at 30 °C for 10 min, reactions were stopped and immunoblotted with anti-Tyr(P) mAb (pSrc), followed by reprobbed with anti-Src Ab. Alignment of Lyn and Src sequences, corresponding to the sequence from which KRX-055_{G106} was derived, are shown. *d*, DU-145 cells were treated with various concentrations of KRX-055_{G106} formulated in AMI159 (◆) for 72 h and cell number was detected using the methylene blue method. Lyn-derived peptide KRX-055_{H213} formulated in AMI159 (□) as well as peptides derived from ERK (○), PDK1 (+, *), or c-Kit formulated in Me₂SO (△) were used for control.

kinase	peptide	sequence	cancerous cell lines					
			HRPC DU-145	HRPC PC-3	Breast MCF-7	Breast MDA-MB-231	Colorectal HT-29	Ovarian A2780
c-Kit	KRX-147 _{D103}	NLLNFLRRK	-	-	-	-	nd	-
Lyn	KRX-055 _{H101}	IVTYGKI	33%	-	-	36%	-	-
Lyn	KRX-055 _{G106}	RTNANVNle	41%	-	-	38%	nd	56%
Fyn	KRX-053 _{H101}	LVTKGRV	-	-	-	-	-	-
Zap-70	KRX-083 _{H104}	LSYGQKPY	-	-	-	-	-	-
Alk-1	KRX-048 _{H101}	GIVEDYRPPF	-	-	-	-	-	-
ILK	KRX-107 _{D115}	GSLYNVLHQGTNF	-	55%	-	25%	-	-
PKB	KRX-014 _{G102}	QGKLFQLIM	49%	-	-	42%	-	52%
PKB	KRX-014 _{H151}	GYNQNHQKLFQL	37%	-	56%	8%	-	41%
PDK1	KRX-702 _{H105}	GRAGNQYL	-	56%	-	-	-	43%
	myr-ethyl-ester		-	-	-	-	nd	nd

FIG. 8. KinScreen array: the inhibitory effect of peptides derived from various kinases on cancerous cell growth. A variety of cancerous cell lines were exposed to 10 different peptides derived from 8 kinases and formulated in Me₂SO or tbi (final 0.1% Me₂SO), except KRX-014_{H151}, which was formulated in AMI159 (detailed under “Experimental Procedures”). After 3–4 days cells were fixed and stained with methylene blue. The percent of cells that survived at 10 μ M peptide relative to those treated by the vehicle is shown when less than 60% survival was detected. 60–100% survival is designated by –, and *nd* stands for non-determined. All peptides are *N*-modified by myristoyl-Gly, and the myristoyl-ethyl ester without the peptidic moiety served as control.

in the hematopoietic system, and particularly in activation of B cells (89).

We show here that two peptides derived from different subregions of the HJ- α G region of Lyn, KRX-055_{H101} and KRX-055_{G106}, potentially inhibited DU-145 and MDA-MB-231 cell proliferation. KRX-055_{H101}, optimized into an HRPC drug candidate KRX-123, was found to be a selective inhibitor of Lyn (24), as well as KRX-055_{G106} (Fig. 7). The novel finding that Lyn is an essential kinase for the viability of DU-145 epithelial cancerous cells, revealed by the KinScreen approach, was subsequently validated: specific inhibition of Lyn expression, using RNA interference, led to reduction in DU-145 cell number,² abnormal expression of Lyn in human prostate cancer samples was detected, and the importance of Lyn to the development of normal prostate gland was displayed (24).

A peptide analogous to KRX-055_{H101}, derived from Src family member Fyn, as well as peptides derived from Zap-70 and Alk-1, showed no inhibitory activity in the array presented in Fig. 8. The above KinScreen array contains a few positive controls. ILK-derived peptide KRX-107_{D115} inhibited the prostate cancer PC-3 and the breast cancer MDA-MB-231 cell proliferation. This result is in agreement with the findings of Yoganathan *et al.* (91) of correlation between increased ILK expression and activity and malignancy in several human tumor types, including breast and prostate carcinomas, and strengthens the notion that ILK might serve as a promising target for these indications.

PKB is implicated in prostate, breast, pancreatic, and ovarian carcinomas as discussed in the previous section. In addition to the inhibition of growth and the biochemical activity of KRX-014_{H151} in the MDA-MB-231 cell line reported above, we assayed proliferation of several cell lines in the presence of KRX-014_{H151} and an additional PKB-derived peptide, KRX-014_{G102}. Indeed, both peptides inhibited cell growth of prostate cancer DU-145, breast cancer MDA-MB-231, and ovarian cancer A2780 cell lines.

PDK1 was suggested as a target for cancer and metabolic diseases. At the cutoff of 10 μ M concentration used for the array described here, we detected inhibition of the prostate cancer PC-3 and the ovarian cancer A2780 cell lines by the PDK1-

derived peptide KRX-702_{H105}. Finally, since our peptides are modified by *N*-myristoylation, we verified that the myristoyl moiety has no inhibitory effect on cell proliferation by itself, utilizing myristoyl-ethyl ester (Fig. 8, *last row*).

DISCUSSION

In this paper we discuss the potential of the KinAceTM regions of kinases, namely the HJ- α G and α D domains (regions X-XI and V, respectively), in substrate recognition and binding. The structural and sequence analysis of the protein kinases revealed well defined templates of these regions, consisting of accessible and variable patches distributed between conserved and buried anchors. The accessible and variable nature of these patches suggests these regions as specificity determinants for protein-protein interactions, and specifically as selective distal substrate binding sites. Indeed, mining of mutational data resulted in multiple cases where these regions were responsible for substrate specificity or for the down-signaling of the kinase. Additional support for a significant involvement of the KinAceTM regions came from the analysis of protein-protein interactions in crystal structures of kinases complexed with peptidic substrates or pseudosubstrates, as well as with auto-inhibitory regions.

The KinAceTM approach presented in this paper takes advantage of the conserved templates to derive short peptides from these regions as modulators of the kinase signaling. Because the kinase-substrate interface may vary among the different kinases, one must derive several peptides, which span the KinAceTM regions. We have derived peptides from KinAceTM regions of two Ser/Thr kinases and two tyrosine kinases, and have shown that these peptides inhibit the signaling of the kinases from which they were derived, whereas control peptides fail to do so. Additional evidence for the utility of KinAceTM peptides as inhibitors of kinase signaling has been provided by Zisman *et al.*³ The authors show that a peptide derived from the α D-region of Jak3 specifically inhibits interleukin-4-induced transphosphorylation of Jak3, without affecting Jak2. The peptide inhibits the proliferation of activated CD4⁺ T cells *in vitro* and *in vivo*, enhances apoptosis of these cells, and inhibits the development of collagen-induced arthritis in mice.

² H. Rubin, I. Stein, M. Goldenberg-Furmanov, I. Wexler, R. Porat, E. Pikarsky, and H. Reuveni, manuscript in preparation.

³ P. Zisman, S. Z. Ben-Sasson, K. Makedonski, S. Nedvetzki, E. Pikarsky, and S. A. Ben-Sasson, manuscript submitted for publication.

Based on these results, we have established the KinAceTM technology for derivation of sequence-based specific kinase inhibitors. Short peptides, which span the KinAceTM regions, are derived and screened for their ability to inhibit the kinase from which they were derived. The most potent peptide inhibitor can be further developed into a drug candidate. Acting via a different mechanism than the ATP mimicking molecules, KinAceTM peptides exhibit selectivity even for the extremely challenging cases, such as Src family kinases (93). We have shown that the Lyn-derived peptide KRX-055_{G106} potently inhibited Lyn activity as opposed to Src activity (Fig. 7). Another active Lyn-derived peptide, KRX-123, was shown to inhibit Lyn without affecting Src family members Fyn and Lck (24). The KinAceTM platform may also prove useful as complementing the ATP-targeted approach in cases of ATP-mimic resistant mutants.

A valuable extension of the KinAceTM platform is the KinScreen technology, in which peptides derived from various kinases are screened for a certain biological activity, to detect novel links between kinases and specific diseases. We exemplified the technology choosing cell proliferation as a relevant biological screening assay for cancer, and showed how Lyn, a kinase known to be involved in hemopoietic systems, emerges as a target for solid tumors. The strength of this approach stems from the fact that the sequence alone suffices for derivation of selective inhibitors. Thus the approach is applicable for kinases without known function or solved crystal structure, as well as for well characterized kinases.

In conclusion, we introduced here two novel technologies, KinAceTM and KinScreen, based on the characterization of specific regions in the catalytic domain that are preserved in all protein kinases. These technologies enable us to derive highly specific inhibitors or modulators that can be used as tools for studying the kinase signaling in biological systems or optimized into drugs, and to identify new target kinases for a selected indication. We are currently analyzing the role of the KinAceTM regions in substrate binding by mutational studies of the HJ- α G and α D regions. Further research is required to establish the mode of action of the KinAceTM peptides.

Acknowledgments—We thank Dr. Eran J. Benjamin for the development of AMI159 formulation, Dr. Tali Yarnitzky for mutational data mining and peptide design, Dr. Sharona Elgavish for peptide design, and Dr. Oren Bogin for discussions of the α D region.

REFERENCES

- Traxler, P. (2003) *Expert Opin. Ther. Targets* **7**, 215–234
- Fabbro, D., Ruetz, S., Buchdunger, E., Cowan-Jacob, S., Fendrich, G., Liebetanz, J., Mestan, J., O'Reilly, T., Traxler, P., Chaudhuri, B., Fretz, H., Zimmermann, J., Meyer, T., Caravatti, G., Furet, P., and Manley, P. (2002) *Pharmacol. Ther.* **93**, 79–98
- Engl, R. A., and Bossemeyer, D. (2002) *Pharmacol. Ther.* **93**, 99–111
- Blum, G., Gazit, A., and Levitzki, A. (2000) *Biochemistry* **39**, 15705–15712
- Lou, Q., Leftwich, M. E., McKay, R. T., Salmon, S. E., Rychetsky, L., and Lam, K. S. (1997) *Cancer Res.* **57**, 1877–1881
- Alfaro-Lopez, J., Yuan, W., Phan, B. C., Kamath, J., Lou, Q., Lam, K. S., and Hruby, V. J. (1998) *J. Med. Chem.* **41**, 2252–2260
- Ramdas, L., Obeyesekere, N. U., Sun, G., McMurray, J. S., and Budde, R. J. (1999) *J. Pept. Res.* **53**, 569–577
- Eichholtz, T., de Bont, D. B., de Widt, J., Liskamp, R. M., and Ploegh, H. L. (1993) *J. Biol. Chem.* **268**, 1982–1986
- Yakymovych, I., Engstrom, U., Grimsby, S., Helden, C. H., and Souchelnytskyi, S. (2002) *Biochemistry* **41**, 11000–11007
- Parang, K., and Cole, P. (2002) *Pharmacol. Ther.* **93**, 145–157
- Sawyer, T. K., Bohacek, R. S., Dalgarno, D. C., Eyermann, C. J., Kawahata, N., Metcalf, C. A., 3rd, Shakespeare, W. C., Sundaramoorthi, R., Wang, Y., and Yang, M. G. (2002) *Mini Rev. Med. Chem.* **2**, 475–488
- Ben-Sasson, S. (January 16, 2001) U. S. Patent 6,174,993
- Zaliani, A., Pinori, M., Ball, H. L., DiGregorio, G., Cremonesi, P., and Mascagni, P. (1998) *Protein Eng.* **11**, 803–810
- Zheleva, D. I., McInnes, C., Gavine, A. L., Zhelev, N. Z., Fischer, P. M., and Lane, D. P. (2002) *J. Pept. Res.* **60**, 257–270
- Ball, K. L., Lain, S., Fahraeus, R., Smythe, C., and Lane, D. P. (1997) *Curr. Biol.* **7**, 71–80
- Adachi, T., Pazdrak, K., Stafford, S., and Alam, R. (1999) *J. Immunol.* **162**, 1496–1501
- Adachi, T., Stafford, S., Sur, S., and Alam, R. (1999) *J. Immunol.* **163**, 939–946
- Kelemen, B. R., Hsiao, K., and Goueli, S. A. (2002) *J. Biol. Chem.* **277**, 8741–8748
- Nichols, A., Camps, M., Gillieron, C., Chabert, C., Brunet, A., Wilsbacher, J., Cobb, M., Pouyssegur, J., Shaw, J. P., and Arkininstall, S. (2000) *J. Biol. Chem.* **275**, 24613–24621
- Scott, J. W., Norman, D. G., Hawley, S. A., Kontogiannis, L., and Hardie, D. G. (2002) *J. Mol. Biol.* **317**, 309–323
- Goldberg, J., Nairn, A. C., and Kuriyan, J. (1996) *Cell* **84**, 875–887
- Akamine, P., Madhusudan, W. J., Xuong, N. H., Eyck, L. F., and Taylor, S. S. (2003) *J. Mol. Biol.* **327**, 159–171
- Bonny, C., Oberson, A., Negri, S., Sauser, C., and Schorderet, D. F. (2001) *Diabetes* **50**, 77–82
- Goldenberg-Furmanov, M., Stein, I., Pikarsky, E., Rubin, H., Kasem, S., Wygoda, M., Weinstein, I., Reuveni, H., and Ben-Sasson, S. A. (2003) *Cancer Res.*, in press
- Licht, T., Tsurulnikov, L., Reuveni, H., Yarnitzky, T., and Ben-Sasson, S. A. (2003) *Blood* **102**, 2099–2107
- Nicosia, R. F., and Ottinetti, A. (1990) *Lab. Invest.* **63**, 115–122
- Strom, S. C., and Michalopoulos, G. (1982) *Methods Enzymol.* **82**, 544–555
- Nissanov, J., Tuman, R. W., Gruver, L. M., and Fortunato, J. M. (1995) *Lab. Invest.* **73**, 734–739
- Hardie, G., and Hanks, S. (eds) (1995) *The Protein Kinase Facts Book*, Vol. II, Academic Press Inc., New York
- Lowe, E. D., Noble, M. E., Skamnaki, V. T., Oikonomakos, N. G., Owen, D. J., and Johnson, L. N. (1997) *EMBO J.* **16**, 6646–6658
- Yang, J., Cron, P., Good, V. M., Thompson, V., Hemmings, B. A., and Barford, D. (2002) *Nat. Struct. Biol.* **9**, 940–944
- Brown, N. R., Noble, M. E., Endicott, J. A., and Johnson, L. N. (1999) *Nat. Cell Biol.* **1**, 438–443
- Favelyukis, S., Till, J. H., Hubbard, S. R., and Miller, W. T. (2001) *Nat. Struct. Biol.* **8**, 1058–1063
- Parang, K., Till, J. H., Ablooglu, A. J., Kohanski, R. A., Hubbard, S. R., and Cole, P. A. (2001) *Nat. Struct. Biol.* **8**, 37–41
- Hubbard, S. R. (1997) *EMBO J.* **16**, 5572–5581
- Gaul, B. S., Harrison, M. L., Geahlen, R. L., Burton, R. A., and Post, C. B. (2000) *J. Biol. Chem.* **275**, 16174–16182
- Knighton, D. R., Zheng, J. H., Ten Eyck, L. F., Xuong, N. H., Taylor, S. S., and Sowadski, J. M. (1991) *Science* **253**, 414–420
- Jones, D. T., Taylor, W. R., and Thornton, J. M. (1991) *Comput. Appl. Sci.* **8**, 275–282
- Kallunki, T., Su, B., Tsigelny, I., Sluss, H. K., Derijard, B., Moore, G., Davis, R., and Karin, M. (1994) *Genes Dev.* **8**, 2996–3007
- Till, J. H., Chan, P. M., and Miller, W. T. (1999) *J. Biol. Chem.* **274**, 4995–5003
- Wen, W., and Taylor, S. S. (1994) *J. Biol. Chem.* **269**, 8423–8430
- Shaltiel, S., Cox, S., and Taylor, S. S. (1998) *Proc. Natl. Acad. Sci. U. S. A.* **95**, 484–491
- Kobe, B., Heierhorst, J., Feil, S. C., Parker, M. W., Benian, G. M., Weiss, K. R., and Kemp, B. E. (1996) *EMBO J.* **15**, 6810–6821
- Hu, S. H., Parker, M. W., Lei, J. Y., Wilce, M. C., Benian, G. M., and Kemp, B. E. (1994) *Nature* **369**, 581–584
- Mayans, O., van der Ven, P. F., Wilm, M., Mues, A., Young, P., Furst, D. O., Wilmanns, M., and Gautel, M. (1998) *Nature* **395**, 863–869
- Shewchuk, L. M., Hassell, A. M., Ellis, B., Holmes, W. D., Davis, R., Horne, E. L., Kadwell, S. H., McKee, D. D., and Moore, J. T. (2000) *Struct. Fold Des.* **8**, 1105–1113
- Herring, B. P., Gallagher, P. J., and Stull, J. T. (1992) *J. Biol. Chem.* **267**, 25945–25950
- Gallagher, P. J., Herring, B. P., Trafny, A., Sowadski, J., and Stull, J. T. (1993) *J. Biol. Chem.* **268**, 26578–26582
- Huang, C. Y., Yuan, C. J., Blumenthal, D. K., and Graves, D. J. (1995) *J. Biol. Chem.* **270**, 7183–7188
- Batkin, M., and Shaltiel, S. (1999) *FEBS Lett.* **452**, 395–399
- Takahashi, Y., Kadowaki, H., Momomura, K., Fukushima, Y., Orban, T., Okai, T., Taketani, Y., Akanuma, Y., Yazaki, Y., and Kadowaki, T. (1997) *Diabetologia* **40**, 412–420
- Desbois-Mouthon, C., Danan, C., Amselem, S., Blivet-Van Eggelpoel, M. J., Sert-Langeron, C., Goossens, M., Besmond, C., Capeau, J., and Caron, M. (1996) *Metabolism* **45**, 1493–1500
- Brotherton, D. H., Dhanaraj, V., Wick, S., Brizuela, L., Domaille, P. J., Volyanik, E., Xu, X., Parisini, E., Smith, B. O., Archer, S. J., Serrano, M., Brenner, S. L., Blundell, T. L., and Laue, E. D. (1998) *Nature* **395**, 244–250
- Chang, C. I., Xu, B. E., Akella, R., Cobb, M. H., and Goldsmith, E. J. (2002) *Mol. Cell* **9**, 1241–1249
- Dasgupta, P., Singh, A. T., and Mukherjee, R. (2000) *Life Sci.* **66**, 1557–1570
- Wettergren, A., Pridal, L., Wojdemann, M., and Holst, J. J. (1998) *Regul. Pept.* **77**, 83–87
- Lauta, V. M. (2000) *Fundam. Clin. Pharmacol.* **14**, 425–442
- Brinckhoff, L. H., Kalashnikov, V. V., Thompson, L. W., Yamshchikov, G. V., Pierce, R. A., Galavotti, H. S., Engelhard, V. H., and Slingluff, C. L., Jr. (1999) *Int. J. Cancer* **83**, 326–334
- Camenisch, G. P., Wang, W., Wang, B., and Borchardt, R. T. (1998) *Pharmacol. Res.* **15**, 1174–1181
- Avdeef, A. (2001) *Curr. Top. Med. Chem.* **1**, 277–351
- Boissan, M., Feger, F., Guillosson, J. J., and Arock, M. (2000) *J. Leukocyte Biol.* **67**, 135–148
- Blume-Jensen, P., Claesson-Welsh, L., Siegbahn, A., Zsebo, K. M., Westermarck, B., and Heldin, C. H. (1991) *EMBO J.* **10**, 4121–4128
- Linnekin, D. (1999) *Int. J. Biochem. Cell Biol.* **31**, 1053–1074
- Blume-Jensen, P., Ronnstrand, L., Gout, I., Waterfield, M. D., and Heldin, C. H. (1994) *J. Biol. Chem.* **269**, 21793–21802
- Blume-Jensen, P., Janknecht, R., and Hunter, T. (1998) *Curr. Biol.* **8**, 779–782

66. Zhang, W., Stoica, G., Tasca, S. I., Kelly, K. A., and Meininger, C. J. (2000) *Cancer Res.* **60**, 6757–6762
67. Vanhaesebroeck, B., and Alessi, D. R. (2000) *Biochem. J.* **346**, 561–576
68. Zeng, X., Xu, H., and Glazer, R. I. (2002) *Cancer Res.* **62**, 3538–3543
69. Wick, K. L., and Liu, F. (2001) *Curr. Drug Targets Immun. Endocr. Metabol. Disord.* **1**, 209–221
70. Bastola, D. R., Pahwa, G. S., Lin, M. F., and Cheng, P. W. (2002) *Mol. Cell. Biochem.* **236**, 75–81
71. Whang, Y. E., Wu, X., Suzuki, H., Reiter, R. E., Tran, C., Vessella, R. L., Said, J. W., Isaacs, W. B., and Sawyers, C. L. (1998) *Proc. Natl. Acad. Sci. U. S. A.* **95**, 5246–5250
72. Kroner, C., Eybrechts, K., and Akkerman, J. W. (2000) *J. Biol. Chem.* **275**, 27790–27798
73. Brazil, D. P., Park, J., and Hemmings, B. A. (2002) *Cell* **111**, 293–303
74. Bellacosa, A., de Feo, D., Godwin, A. K., Bell, D. W., Cheng, J. Q., Altomare, D. A., Wan, M., Dubeau, L., Scambia, G., Masciullo, V., Ferrandina, G., Benedett Panici, P., Mancuso, S., Neri, G., and Testa, J. R. (1995) *Int. J. Cancer* **64**, 280–285
75. Nakatani, K., Thompson, D. A., Barthel, A., Sakaue, H., Liu, W., Weigel, R. J., and Roth, R. A. (1999) *J. Biol. Chem.* **274**, 21528–21532
76. Testa, J. R., and Bellacosa, A. (2001) *Proc. Natl. Acad. Sci. U. S. A.* **98**, 10983–10985
77. Stambolic, V., Mak, T. W., and Woodgett, J. R. (1999) *Oncogene* **18**, 6094–6103
78. Alessi, D. R., Andjelkovic, M., Caudwell, B., Cron, P., Morrice, N., Cohen, P., and Hemmings, B. A. (1996) *EMBO J.* **15**, 6541–6551
79. Franke, T. F., Yang, S. I., Chan, T. O., Datta, K., Kazlauskas, A., Morrison, D. K., Kaplan, D. R., and Tsichlis, P. N. (1995) *Cell* **81**, 727–736
80. Jackson, J. G., Kreisberg, J. I., Koterba, A. P., Yee, D., and Brattain, M. G. (2000) *Oncogene* **19**, 4574–4581
81. Zhang, X., Gan, L., Pan, H., Guo, S., He, X., Olson, S. T., Mesecar, A., Adam, S., and Unterman, T. G. (2002) *J. Biol. Chem.* **277**, 45276–45284
82. Burgering, B. M., and Kops, G. J. (2002) *Trends Biochem. Sci.* **27**, 352–360
83. Graff, J. R., Konicek, B. W., McNulty, A. M., Wang, Z., Houck, K., Allen, S., Paul, J. D., Hbailu, A., Goode, R. G., Sandusky, G. E., Vessella, R. L., and Neubauer, B. L. (2000) *J. Biol. Chem.* **275**, 24500–24505
84. Bolen, J. B., Rowley, R. B., Spana, C., and Tsygankov, A. Y. (1992) *FASEB J.* **6**, 3403–3409
85. Atfi, A., Drobetsky, E., Boissonneault, M., Chapdelaine, A., and Chevalier, S. (1994) *J. Biol. Chem.* **269**, 30688–30693
86. Sumitomo, M., Shen, R., Walburg, M., Dai, J., Geng, Y., Navarro, D., Boileau, G., Papandreou, C. N., Giancotti, F. G., Knudsen, B., and Nanus, D. M. (2000) *J. Clin. Invest.* **106**, 1399–1407
87. Allard, P., Atfi, A., Landry, F., Chapdelaine, A., and Chevalier, S. (1997) *Mol. Cell. Endocrinol.* **126**, 25–34
88. Varadarajan, S., Yatin, S., Kanski, J., Jahanshahi, F., and Butterfield, D. A. (1999) *Brain Res. Bull.* **50**, 133–141
89. Fujimoto, M., Fujimoto, Y., Poe, J. C., Jansen, P. J., Lowell, C. A., DeFranco, A. L., and Tedder, T. F. (2000) *Immunity* **13**, 47–57
90. Chan, V. W., Meng, F., Soriano, P., DeFranco, A. L., and Lowell, C. A. (1997) *Immunity* **7**, 69–81
91. Yoganathan, N., Yee, A., Zhang, Z., Leung, D., Yan, J., Fazli, L., Kojic, D. L., Costello, P. C., Jabali, M., Dedhar, S., and Sanghera, J. (2002) *Pharmacol. Ther.* **93**, 233–242
92. Deleted in proof
93. Karni, R., Mizrahi, S., Reiss-Sklan, E., Gazit, A., Livnah, O., and Levitzki, A. (2003) *FEBS Lett.* **537**, 47–52
94. Paradis, S., Ailion, M., Toker, A., Thomas, J. H., and Ruvkun, G. (1999) *Genes Dev.* **13**, 1438–1452
95. Fleig, U. N., Gould, K. L., and Nurse, P. (1992) *Mol. Cell. Biol.* **12**, 2295–2301
96. Robinson, F. L., Whitehurst, A. W., Raman, M., and Cobb, M. H. (2002) *J. Biol. Chem.* **277**, 14844–14852
97. Lei, M., Lu, W., Meng, W., Parrini, M. C., Eck, M. J., Mayer, B. J., and Harrison, S. C. (2000) *Cell* **102**, 387–397
98. Yokoyama, N., and Miller, W. T. (1999) *FEBS Lett.* **456**, 403–408
99. Krueger, J. K., Padre, R. C., and Stull, J. T. (1995) *J. Biol. Chem.* **270**, 16848–16853
100. Tanoue, T., Maeda, R., Adachi, M., and Nishida, E. (2001) *EMBO J.* **20**, 466–479